COMPRESSION AND BUCKLING OF RODS IN CREEP UNDER MONOTONICALLY INCREASING LOADS

O. V. Sosnin and N. G. Torshenov

Zhurnal Prikladnoi Mekhaniki i Tekhnicheskoi Fiziki, Vol. 8, No. 5, pp. 140–144, 1967

Experimental data are presented on the compression of rods in creep under loads increasing at a constant rate. A method of determining the creep characteristics of materials under these conditions is described and the results are compared with characteristics determined by creep tests under constants loads. The results of buckling tests on axially compressed hinged rods are described and the calculated values of critical loads (for the same loading conditions) obtained by certain engineering methods are given.

§1. Alloy D16T rod specimens (14 mm diameter) were used in the experiments conducted at a constant temperature of 250 ± 2° C at four loading rates in range 4.5–0.0045 kgf/mm^2·sec. The specimen gauge portion was 7 ± 0.01 mm in diameter and 40 ± 0.1 mm long in compression tests and 62–142 mm long in buckling tests. All the specimens were made from material as delivered and were not subjected to any heat treatment. The testing machine and experimental technique are described in [1].

The starting hypothesis was that instantaneous elastoplastic strains and time-dependent creep strains are not related to each other, i.e., that the total strain ε may be represented as the sum

$$\varepsilon = w(\sigma) + p, \tag{1.1}$$

where the first term on the right-hand side is the instantaneous elastoplastic strain and the second term is the creep strain which can be described by

$$p^{\alpha} dp = K e^{\beta\sigma} dt. \tag{1.2}$$

Here α, K, and β denote experimentally determined material characteristics, σ is stress and t is time. When the load monotonically increases with time at rate c, the creep strain—after integrating (1.2)—will be described by

$$p^{\alpha+1} = \frac{(1+\alpha)K}{\beta c}(e^{\beta c t} - 1). \tag{1.3}$$

It is seen from (1.3) that creep strain decreases with increasing loading rate and that, starting from a certain rate $c \geq c_0$, the creep strain does not exceed the magnitude of the scatter of experimental points on an ordinary creep curve $\sigma(\varepsilon)$. Thus, at loading rates faster than 3 kgf/mm^2·sec all the curves $\sigma(\varepsilon)$ merge to form a narrow band in both the elastic and plastic ranges; one may therefore conclude that virtually no creep strain is produced at these loading rates. Diagrams in which phenomena associated with time are not reflected are called instantaneous [2].

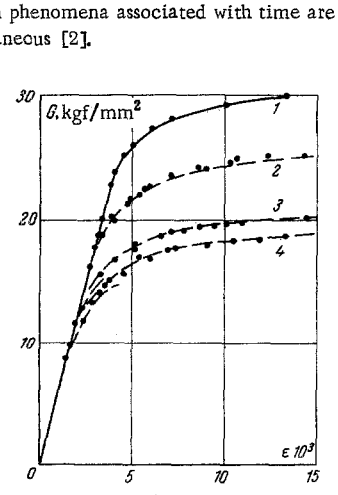

Fig. 1

Curves $\sigma(\varepsilon)$ for rods in compression are shown in Fig. 1, where the numbers 1, 2, 3, and 4 indicate loading rates of 4.5, 0.2, 0.01, and 0.0045 kgf/mm^2·sec, respectively. It will be seen that, irrespective of the loading rate applied, no creep strain is produced at stresses below 8 kgf/mm^2; the deformation process is elastic in character, the elasticity modulus E being equal to $5.6 \cdot 10^3$ kgf/mm^2.

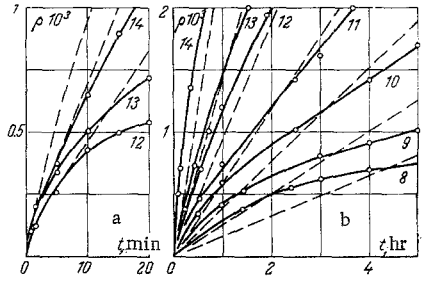

Fig. 2

At higher stresses diagrams obtained at slow loading rates deviate from curve 1 (instantaneous diagram) the difference representing the accumulated creep strain; the divergence of the fan of curves $\sigma(\varepsilon)$ considerably increases with decreasing loading rate. In a loading-rate range on the order of 10^{-1} kgf/mm^2·sec, which is of practical interest, the difference in the $\sigma(\varepsilon)$ curves becomes marked when the loading rate is reduced or increased by a factor of 3–4. As a result, it is possible in these loading–rate intervals to use a linear mode of load increase as an approximation of any monotonically increasing loading path which considerably simplifies the analysis of experimental results.

The material creep characteristics can be obtained from Eq. (1.2) by analyzing experimental data in Fig. 1 in the following way. Measuring the creep strains p_j and p_k along a horizontal line corresponding to a certain stress σ_i, for the distances between the instantaneous diagram and diagrams for the loading rates c_j and c_k, respectively, and successively substituting these values into (1.3), we obtain

$$(p / p_k)^{\alpha+1} = c_k / c_j, \tag{1.4}$$

from which the strengthening coefficient α can be determined. The analysis of experimental data showed that α decreases monotonically from 0.3 at a stress of 12 kgf/mm^2 to zero at a stress of 15 kgf/mm^2 or more. This is in good agreement with the results of tests at constant loads which showed that at high stress levels the material studied behaves like a nonhardening medium.

If stresses σ_j and σ_k corresponding to equal strains $p_j = p_k$ produced at different loading rates c_j and c_k are determined and substituted into (1.3), and if the right sides are equated, we obtain

$$c_j^{-1}(\exp \beta\sigma_j - 1) = c_k^{-1}(\exp \beta\sigma_k - 1), \tag{1.5}$$

from which β can be found. This coefficient is not a constant material property either: as the stress increases from 10 to 20 kgf/mm^2, β monotonically increases in the interval $0.4 \leq \beta \leq 0.9$ mm^2/kgf. analogously, if equation

$$p^{\alpha} dp = B\sigma^n dt, \tag{1.6}$$

is used instead of (1.2), we find that the exponent n in the above stress range varies in the interval $4 \leq n \leq 11$. Hence follows that relations (1.2) and (1.6) may be used to describe creep only in a very narrow stress interval and that, generally speaking, the stress dependence of creep is stronger than that described by power (1.6) or exponential (1.2) functions.

If α and β are known and if strains corresponding to various loading rates are determined, Eq. (1.3) can be used to determine K (taking its mean value). In view of the wide variation in α and β, it is advisable (for the purpose of further analysis) to divide the entire stress interval into two ranges for each of which the values of α, β, and K are then averaged. Thus, we took

$$\text{for } \sigma > 14 \text{ kgf/mm}^2,$$

$$\alpha = 0, \quad \beta = 0.6 \text{ mm}^2/\text{sec}, \quad K = 3.4 \cdot 10^{-10} \text{ sec}^{-1}; \qquad (1.7)$$

$$\text{for } \sigma \leqslant 14 \text{ kgf/mm}^2,$$

$$\alpha = 0.13, \quad \beta = 0.44 \text{ mm}^2/\text{sec}, \quad K = 13.2 \cdot 10^{-10} \text{ sec}^{-1}. \qquad (1.8)$$

Diagrams constructed with the aid of (1.3) and using constants for the appropriate stress intervals and loading rates are plotted in Fig. 1 and are shown as dashed lines which coincide rather well with the experimental points.

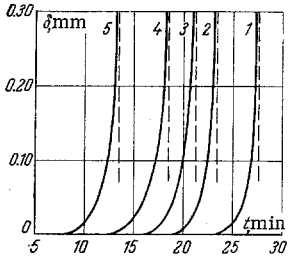

Fig. 3

In this context it is interesting to compare the results obtained with experimental data on the creep of the alloy in question under constant loads. It was shown in [3] that the creep properties of D16 alloy in tension and compression are the same and they were therefore compared with experimental results obtained for identical specimens tested at the same temperatures and at stresses ranging from 8 to 15 kgf/mm^2 which correspond to the stress interval in which the creep is described by the characteristics of (1.8). It was found that curves plotted from (1.2) using the characteristics of (1.8) run considerably above the experimental points, coinciding with the latter only in the first few minutes.

The solid lines in Fig. 2a represent experimental creep curves obtained at stresses indicated by the numbers on each curve (in kgf/mm^2), while the dashed lines represent calculated curves obtained with the aid of Eq. (1.2). The picture presented by Fig. 2a is not unexpected, since it is known that changing the stress σ to a higher level is, in the case of hardening materials, accompanied by a substantial increase in the intensity of creep at the instant at which the stress is increased [4]; this effect is not described by the hypothesis of strain hardening (1.2) and (1.6). When the load is monotonically increased, this intensification of creep will take place continuously. Thus, if creep characteristics are obtained from experimental data relating to increasing stress and applied to describe the creep at constant loads, overestimated values will be obtained; conversely, using experimental data relating to constant loads will produce underestimated (in comparison with experiment) values. The latter is quite an important consideration since it means that using characteristics obtained by experiments at constant loads will lead to errors on the dangerous side (i.e., to underestimating the effects of real processes under variable loads).

If α is assumed to be equal to zero with β and K remaining unchanged and if Eq. (1.3) is used again to describe the creep at constant loads in the same stress interval, it is found that the calculated curves on the whole encompass the process almost to the beginning of its third stage. Curves of this kind are shown in Fig. 2b (dashed lines) with the solid lines representing experimental data obtained at the stresses (kgf/mm^2) indicated by the numbers.

It follows from the above results that creep characteristics in Eqs. (1.2) and (1.6) usually determined by experiments at constant loads give only a very approximate picture of the real processes taking place at variable loads even in the case of such materials as the one cited above which do not appreciably harden; it is obvious that in the case of materials whose creep is accompanied by a more intense hardening, the discrepancy may be even larger.

§2. The above cited creep characteristics of the material increasing loads were used to analyze experimental data on the buckling of hinged cylindrical specimens operating at the same temperature and under the same loading conditions. To ensure a hinged support, steel ferrules were fitted onto the specimen ends; the length of the specimen pushed into the ferrule with a sliding fit was equal to the specimen diameter. The ferrules had prismatic grooves (with an angle of 120°) for hinged support, while the location of the groove relative to the geometric axis of the specimen determined the degree of centricity of the applied load transmitted through the knife edges of the push-rods; the knife-edges had an angle of 75° and a radius of less than 0.01 mm.

The tests were carried out on five batches of specimens of various length corresponding to the following flexibilities: $\lambda_1 = 35$, $\lambda_2 = 47$, $\lambda_3 = 58$, $\lambda_4 = 70$ and $\lambda_5 = 81$; the specimen gauge portion was taken to be equal to the distance between the knife edges on the push-rods which was 2 mm larger than the specimen gauge length.

In the processing of experimental data only those experiments were used in which the initial eccentricity of the applied load was close to its technically lowest possible value (not more than a few microns) and in which the bending deflection started to increase when the increasing load reached a level on the order of 75% of the breaking stress (virtually independent of the loading rate) and at stresses at which creep should come into play. The stress at which the bending deflection started to increase (average value of several test results) was taken as the critical stress σ^*, the breaking stress σ^{**} being that corresponding to unlimited increase in the bending deflection.

Typical curves representing the time dependence of the bending deflection at loading rates on the order of 0.18 kgf/mm^2·sec are shown in Fig. 3, where the numbers indicated the flexibility (in the order of values cited above). The dashed line next to each curve corresponds to the time-to-rupture of a given specimen. Qualitatively analogous diagrams were obtained (for the same test temperature and flexibility range) at other loading rates.

The experimental data were compared with calculated results obtained from certain semiempirical formulas used to estimate the critical stresses and time-to-rupture values of thin-walled columns in creep under constant loads [5, 8].

λ	c	σ_1		σ_2		σ_3		σ^*	σ^{**}
1	2	3	4	5	6	7	8	9	10
35	3.7500	23.9		28.2		25.0		24.4	26.0
	0.1920	19.7		23.5		20.6		21.0	23.8
	0.0112	15.5		19.1		16.5		15.4	17.8
	0.0050	14.4		17.8		15.4		15.0	16.5
47	3.4600	21.1		23.7		21.9		20.0	22.8
	0.1630	17.5		20.6		18.4		18.8	20.8
	0.0115	14.1	13.9	17.1	17.0	15.0	15.1	13.8	16.0
	0.0046	12.9	12.4	15.8	15.6	13.8	13.7	12.8	14.6
58	4.5000	16.3		16.4		16.4		16.7	18.3
	0.1810	15.1	14.9	16.1	16.0	15.5	15.4	13.0	16.3
	0.0117	12.6	12.0	14.6	14.5	13.3	12.9	11.7	14.1
	0.0046	11.5	10.7	13.8	13.0	12.3	11.8	11.2	12.8
70	3.4600	11.3	11.2	11.3	11.2	11.3	11.2	11.2	13.7
	0.2200	11.2	11.2	11.2	11.2	11.2	11.2	9.3	13.3
	0.0108	10.4	9.7	11.1	10.6	10.7	10.2	8.8	11.9
	0.0046	9.8	8.9	10.8	10.2	10.3	9.6	8.4	11.0
81	3.4600	8.4	8.4	8.4	8.4	8.4	8.4	7.0	10.2
	0.2080	8.4	8.4	8.4	8.4	8.4	8.4	6.0	9.4
	0.0110	8.2	7.8	8.4	8.2	8.3	8.1	6.0	9.2
	0.0044	8.0	7.3	8.3	7.9	8.2	7.8	5.7	9.0

In accordance with [5, 6] it is postulated that a straight rod will start to bend after an infinitely small disturbance, when the following condition is satisfied;

$$\sigma = \pi^2 E_t / \lambda^2, \qquad (2.1)$$

where E_t is the tangent modulus drawn to an isochronous curve $\sigma(\varepsilon)$ at a point corresponding to a certain fixed time which appears as a parameter in the family of curves $\sigma(\varepsilon)$.

When we have to determine the critical stress for a rod carrying a monotonically increasing load, it is natural to take the loading rate as the parameter of the family of curves $\sigma(\varepsilon)$ and to calculate E_t from the parametric curve corresponding to this rate. Taking into account Eqs. (1.1) and (1.3), we obtain

$$\frac{1}{E_t} = \frac{d\varepsilon}{d\sigma} = \frac{1}{E} + \frac{K}{c} e^{\beta\sigma} \left[\frac{(\alpha+1)K}{\beta c}(e^{\beta\sigma}-1)\right]^{-\alpha/(\alpha+1)}. \quad (2.2)$$

Substituting the value of E_t obtained from (2.2) into (2.1), we obtain an equation for determining the critical stress σ corresponding to a given loading rate c

$$\sigma\left[1 + \frac{EK}{c} e^{\beta\sigma}\left\{\frac{(\alpha+1)K}{\beta c}(e^{\beta\sigma}-1)\right\}^{-\alpha/(\alpha+1)}\right] = \frac{\pi^2 E}{\lambda^2}. \quad (2.3)$$

Values of σ_1 calculated from Eq. (2.3) using the averaged characteristics of (1.7) are given in the third column of the table; values of σ_1 obtained from (2.3) using the characteristics of (1.8) are given in column 4. Since the characteristics of (1.7) slightly underestimate the real creep strain corresponding to stresses of 14 kgf/mm^2 or more, the critical stresses calculated with the aid of these characteristics are somewhat higher than those calculated with the aid of the characteristics in (1.8); this obviously applies also to other criteria.

According to [7] it is postulated that the total strain at which a straight rod will start to bend in creep should be the same as that at which the rod would buckle under normal loading conditions

$$\varepsilon_* = \varepsilon^0 + p = \pi^2/\lambda^2. \quad (2.4)$$

Hence, taking into account Eq. (1.3), we obtain an equation for determining the critical stress corresponding to a given loading rate

$$\sigma + E\left\{\frac{(\alpha+1)K}{\beta c}(e^{\beta\sigma}-1)\right\}^{1/(\alpha+1)} = \frac{\pi^2 E}{\lambda^2}. \quad (2.5)$$

Values of σ_2 calculated from Eq. (2.5) using the characteristics of (1.7) and (1.8) are given in the table, in columns 5 and 6, respectively.

If the lateral disturbance is applied sufficiently fast so that the outer "fibers" of the rod during bending are slightly relieved (despite the active axial load), taking this into account in the determination of the critical stress leads to the concept of effective modulus. Since the latter depends not only on E and E_t but also on the moment of inertia of the rod cross section, a simplified method of calculation was applied by using an ideal "I" cross section for the rod instead of its real cross section in estimating the effective modulus of rod core. In this case, after substituting the effective modulus

$$E^{**} = 2EE_t/(E+E_t), \quad (2.6)$$

for E_t into the expression for the critical stress (2.1) and after some simple transformations, we obtain the following equation for determining the critical stress corresponding to a given loading rate:

$$\frac{\pi^2 E}{\lambda^2} = \sigma\left[1 + \frac{EK}{2c} e^{\beta\sigma}\left\{\frac{(\alpha+1)K}{\beta c}(e^{\beta\sigma}-1)\right\}^{-\alpha/(\alpha+1)}\right]. \quad (2.7)$$

The corresponding values of σ_3 calculated from (2.7) using the characteristics of (1.7) and (1.8) are given in the table, in columns 7 and 8, respectively.

Columns 9 and 10 in the table give the experimental values of the critical (σ^*) and breaking (σ^{**}) stresses. It will be seen that as the flexibility of the rod increases, σ^* and σ^{**} become less markedly dependent on the loading rate, so that the critical stress of rod with $\lambda \geq 70$ may be estimated without taking creep into account.

The dependence of the critical stress on λ for two different loading rates (4.5 and 0.0045 kgf/mm^2·sec) is shown in Fig. 4.

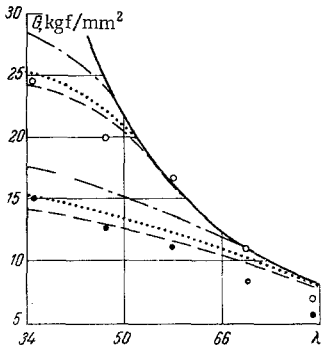

Fig. 4

The solid line represents the Euler hyperbola; the dashed lines represent curves calculated from Eq. (2.3), the dot-dash lines representing curves calculated from Eq. (2.5) and the dotted lines representing the curves calculated from Eq. (2.7). Both families of curves were constructed for the characteristics of (1.7). Open circles in Fig. 4 denote experimental values of σ^* (from the table) in relation to λ at loading rates of several kgf/mm^2·sec, the corresponding values of σ^* obtained at loading rates on the order of 10^{-3} kgf/mm^2·sec being represented by the black circles. Qualitatively analogous families of curves are obtained for other loading rate intervals.

Data reproduced in the table and in Fig. 4 show that, in all the intervals of the axial loading rate and rod flexibility studied, curves calculated with the application of the tangent modulus are closest to the experimental data; curves calculated from the criterion ε = const deviate more from experiment, the deviation being even more pronounced in the case of curves calculated with the application of the effective modulus; in the last two cases the deviation is in the dangerous direction, giving critical stress values higher than those determined by experiment.

REFERENCES

1. N. G. Torshenov, "Machine for column creep buckling tests," Zavodskaya laboratoriya, no. 12, 1964.

2. S. T. Mileiko and V. I. Telenkov, "Short-time creep of aluminum alloys," PMTF, no. 5, 1962.

3. N. G. Torshenov, "Creep of an aluminum D16T alloy in compression," PMTF, no. 6, 1961.

4. V. S. Namestnikov and A. A. Khvostunkov, "Creep of aluminum at constant and variable loads," PMTF, no. 4, 1960. 1960.

5. F. R. Shenli, Analysis of the Weight and Strength of Aircraft Structures [in Russian], Oborongiz, 1957.

6. R. Carlson, "Time-dependent tangent modulus applied to column creep buckling," J. Appl. Mech., vol. 23, no. 3, 1956.

7. G. Gerard, "A creep buckling hypothesis," J. Aeronaut. Sci., vol. 19, no. 10, 1952.

8. N. Hoff, "Review of theories of buckling in creep," collection: Mekhanika [Russian translation], no. 1, 1960.

9 July 1966 Novosibirsk